GPS signal enhancement and attitude determination for a mini and low-cost unmanned aerial vehicle

Ben Yun[1], Guowei Cai[1], Ben M. Chen[1], Kemao Peng[2] and Kai Yew Lum[2]

[1]Department of Electrical and Computer Engineering, National University of Singapore
[2]Temasek Laboratories, National University of Singapore

We present in this paper an integration scheme of a low-cost inertial attitude and position reference system for a mini unmanned helicopter by utilizing the robust and H_∞ filtering technique. The result has been successfully implemented and tested on our mini-scale unmanned helicopter. Simulation and flight experiment results show that the proposed technique is very effective in real-time and suitable for control, stabilization and navigation for mini-scale unmanned air vehicles.

Key words: unmanned aerial vehicles; attitude reference systems; H_∞ filtering

1. Introduction

Unmanned air vehicles (UAVs) have become increasingly popular and are more widely used in both military and civil applications nowadays. They are employed to perform autonomously the wide spectrum of missions that are either dangerous or not feasible by using other means. Owing to the nature of the applications of the UAV systems, which have a trend of moving towards mini and micro scales in size, there is often a tradeoff between the cost and the performance of the UAV that should be constructed. A good design would thus have to yield the best possible performance with a limited budget.

10.1177/0142331209342220

The attitude and heading reference system (AHRS) is one of the most important elements in UAVs. It consists of necessary sensors to provide measurement signals in the body coordinate. Typical sensors used to form an AHRS in the UAVs are accelerometers to measure the accelerations along the three axes of the UAV body coordinate, gyroscopes to provide the three-axis angular rates, and magnetometers to capture the magnet values of the three axes, and some sensors to provide reliable position and velocity information of the UAV for navigation, trajectory tracking, autonomous flight control, and mission completion. In this work, we investigate the integration of low-cost inertial sensors to form an effective AHRS for a mini UAV helicopter. To obtain accurate position and navigation signals, we employ a GPS sensor unit together with an inertial navigation system (INS), which are capable of providing position and orientation information of the UAV. Unfortunately, performance obtained from low-cost inertial sensors available in the market is pretty poor due to error sources such as random noise, biases and scale factor errors. Even though an expensive and bulky INS is able to provide accurate navigation data, its performance degrades gradually with time (see, for example, Britting (1971) and Tsach *et al.* (2002)). Similarly, navigation data generated by GPS sensors carry bounded errors. The GPS signals for positions available for public use only have an accuracy of about 3 m with a sampling frequency of 4 Hz. The velocities, determined from the Doppler effect, have an accuracy of about 0.3 m/s. These measurement errors are rather poor for mini-scale UAVs flying at low speed. As such, it is necessary to introduce some filtering schemes to smooth and improve the GPS measurements for control purpose and for the attenuation of high-frequency noises.

A number of approaches have been introduced recently to improve the performance of GPS and low-cost INS integration. For example, Nassar *et al.* (2004) have investigated the improvement of the accuracy of an inertial measurement unit (IMU) using an autoregressive modelling approach. Different integration filters have also been investigated in the literature. For instance, Shin and El-Sheimy (2002) and van der Merwe and Wan (2004) have studied the use of unscented Kalman filters and Noureldin *et al.* (2004) have considered solutions using neural networks. More traditional approaches of improving the measurement accuracy of GPS and low-cost INS reported in the literature include increasing the number of measurements used in the Kalman filter. The goal of this paper is to present an integration of a low-cost inertial attitude and position reference system for a mini UAV helicopter by utilizing the robust and H_∞ filtering technique. We note that the attitude determination problem is non-linear in nature and its measurement noise is unknown. As such, it is more sensible to linearize the non-linear system and formulate it as an H_∞ filtering problem with the linearization error being treated as system disturbances. Our result has been successfully implemented and tested on our mini-scale UAV helicopter.

The outline of this paper is as follows. Section 2 presents the background on all of the necessary parameters involved in the attitude determination and position enhancement of unmanned vehicles. Section 3 gives details of the setup and

application of the H_∞ filtering technique for the problem we tackle in this work. Section 4 presents the resulting experimental results from actual flight tests. Finally, we draw some concluding remarks in Section 5.

2.   Determination of aircraft position and attitude

In this section, we outline an aircraft position and attitude determination framework, which is to be used for further H_∞ filtering design in the next section.

2.1   Position signals

Let us start with the problem that motivates us to carry out such an enhancement. During the flight tests of our UAV helicopter, we have constantly experienced some unexpected jumps in position signals received from the GPS receiver (see Figure 1). However, we have never observed such jumps occurred in the actual system or even from the velocity signals measured (also see Figure 1). Since the GPS velocity signals received are relatively more accurate compared with those of GPS positions, in principle, we wish to evaluate whether the GPS velocity could provide a reasonably accurate position reference by simply integrating three-axis velocity. However, due to some unknown slow-varying bias, such a simple integration generally results large errors with a large time frame. Figure 2 shows the comparison of the GPS position signals and the results calculated through integration.

Such a problem that we have encountered in experimental testing of our UAV helicopter suggests that there is a need to process the raw data received from the GPS in order to improve the quality of signals received and the overall performance of our flight control systems. In what follows, we derive a set of equations, which can be utilized for the reconstruction of the position signals through the integration of filtered velocities with corrections-based position signals received from the GPS receiver.

Normally, in practical situations, the measurement noise can be modelled as a white noise. Furthermore, there is some low-frequency bias contained in the measured position values. Based on this situation, we can describe the GPS-measured velocity signal v_x as follows

$$v_x = v_x^* + b_x + w_x \tag{1}$$

where v_x^* is the true velocity, b_x is a slow varying bias and w_x is the white noise. The corresponding position can then be computed as

$$p_x = \int v_x \, \mathrm{d}t = \int (v_x^* + b_x + w_x) \, \mathrm{d}t = p_x^* + \int (b_x + w_x) \, \mathrm{d}t \tag{2}$$
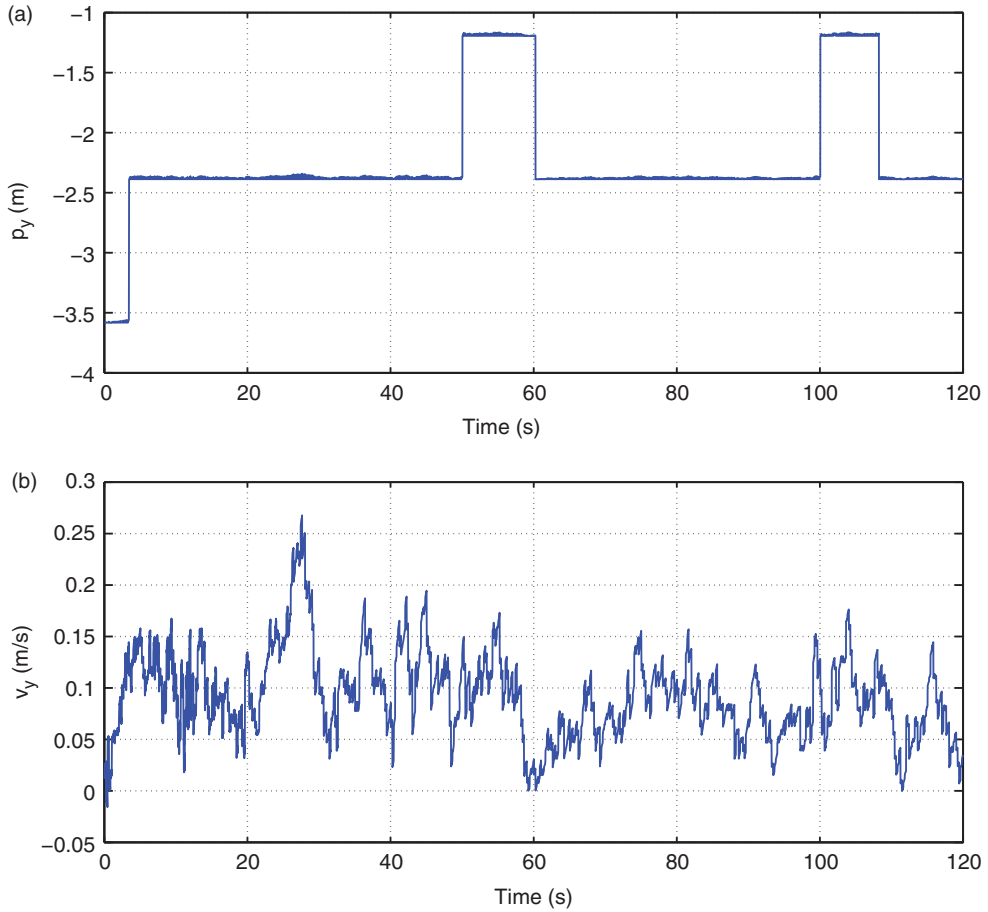
Figure 1 The GPS-measured body-frame y-axis (a) position and
(b) velocity during a hovering flight

where p_x^* is the true position. Noting that b_x is a slow varying variable, we take it as an unknown constant with appropriate noise, i.e.

$$\dot{b}_x = w_b \tag{3}$$

where w_b is assumed to be a white noise. Define e_x to be the position error, i.e. $e_x = p_x - p_x^*$. It follows from (2) that

$$e_x = \int (b_x + w_x)\, \mathrm{d}t \tag{4}$$

and, thus,

$$\dot{e}_x = b_x + w_x \tag{5}$$
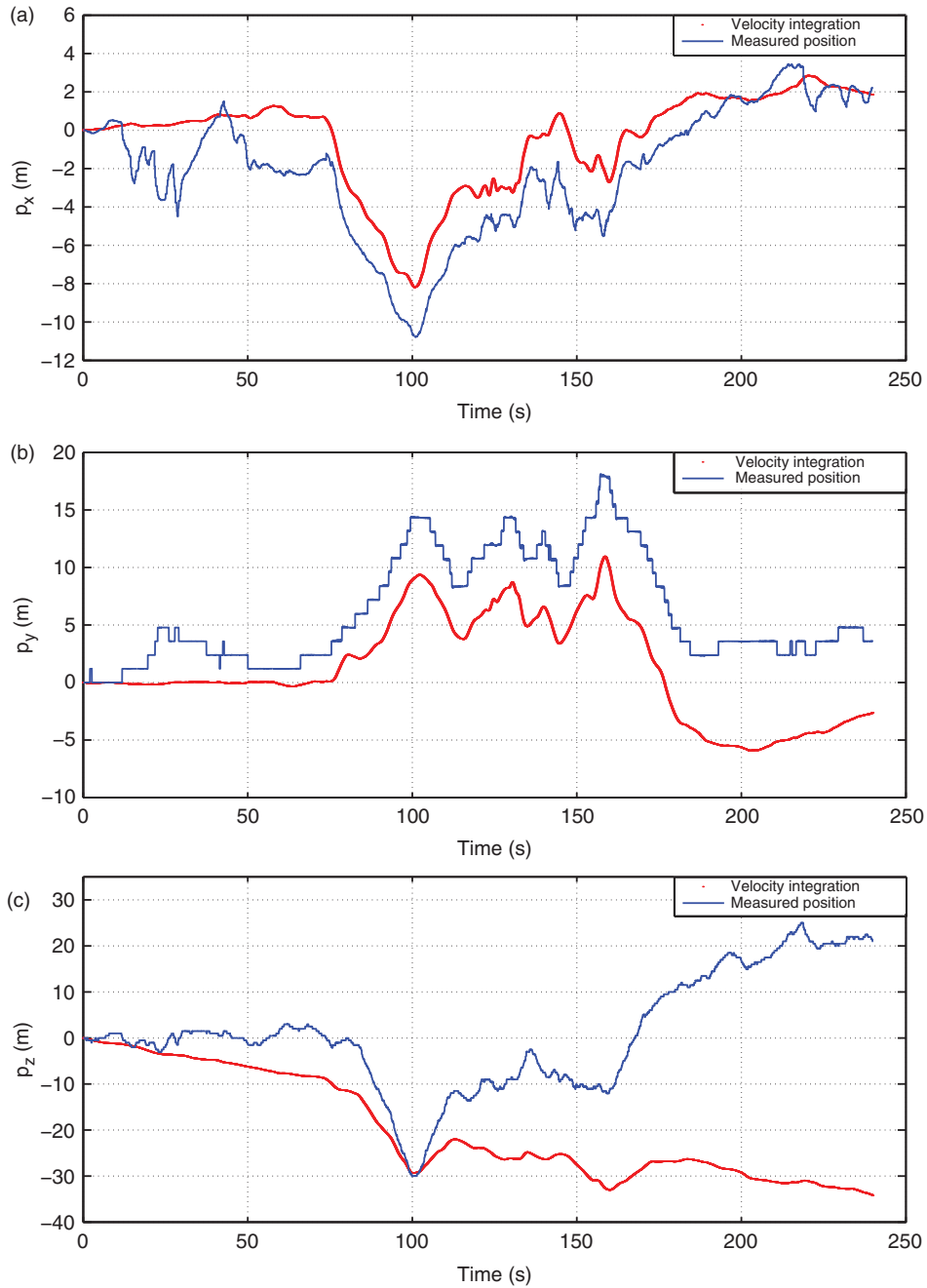
Figure 2 The position integrated by velocity (bold line) and that measured by GPS receiver (thin line): (a) body-frame *x*-axis position signal; (b) body-frame *y*-axis position signal; (c) body-frame *z*-axis position signal

670 GPS signal enhancement and attitude

Next, consider the received position signal, i.e.

$$p_{x,\text{gps}} = p_x^* + n_x \tag{6}$$

where n_x is the position measurement noise. We rewrite

$$p_{x,\text{gps}} = (p_x - e_x) + n_x = p_x - e_x + n_x \tag{7}$$

Defining a measurement output $y = p_x - p_{x,\text{gps}}$, we have

$$y = e_x - n_x \tag{8}$$

Putting (3) and (5) into a matrix form, we have

$$\dot{x} = \begin{bmatrix} 0 & 1 \\ 0 & 0 \end{bmatrix} x + w \tag{9}$$

where

$$x = \begin{pmatrix} e_x \\ b_x \end{pmatrix} \quad \text{and} \quad w = \begin{pmatrix} w_x \\ w_b \end{pmatrix} \tag{10}$$

The measurement output can then be written as

$$y = \begin{bmatrix} 1 & 0 \end{bmatrix} x - n_x \tag{11}$$

We combine (9) and (11) together for single-axis position determination. It should be noted that the above formulation is applicable for all three axes of the aircraft.

2.2 Euler angles

A set of the so-called normal Euler angles are commonly used to describe the orientation of an aircraft. There are three Euler angles, which include the heading or yaw angle (ψ), pitch angle (θ) and roll angle (ϕ). These angles are referenced to the local horizontal plane which is perpendicular to the Earth's gravitational vector as depicted in Figure 3. Heading is defined as the angle in the local horizontal plane measured clockwise from a true north (Earth's polar axis) direction. Pitch is defined as the angle between the aircraft's longitudinal axis and the local horizontal plane (positive for nose up). Roll is defined as the angle about the longitudinal axis between the local horizontal plane and the actual flight orientation (positive for right wing down); see, for example, Caruso (1997, 2000). We note that in Figure 3, (X_{NED}, Y_{NED}, Z_{NED}) and (X_{ABC}, Y_{ABC}, Z_{ABC}) represent respectively the north–east–downward coordinate and the aircraft body coordinate.

The attitude dynamics of the aircraft can be described as (see, for example, Wertz (1978)):

$$\dot{q} = \Omega(\omega)q \tag{12}$$
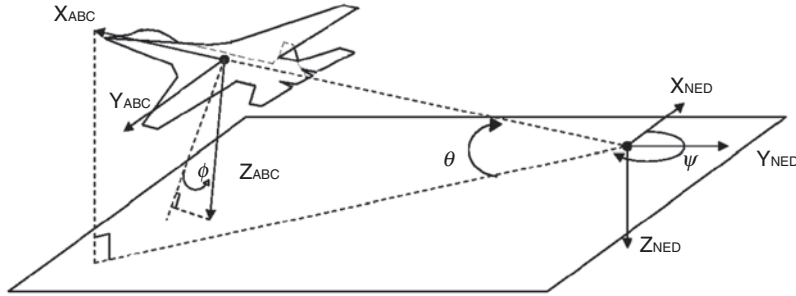
Figure 3 Definition of normal Euler angles

where q is the attitude quaternion vector given by

$$q = \begin{pmatrix} q_0 \\ q_1 \\ q_2 \\ q_3 \end{pmatrix} \qquad (13)$$

with

$$q_0 = \cos\frac{\phi}{2}\cos\frac{\theta}{2}\cos\frac{\psi}{2} + \sin\frac{\phi}{2}\sin\frac{\theta}{2}\sin\frac{\psi}{2} \qquad (14)$$

$$q_1 = \sin\frac{\phi}{2}\cos\frac{\theta}{2}\cos\frac{\psi}{2} - \cos\frac{\phi}{2}\sin\frac{\theta}{2}\sin\frac{\psi}{2} \qquad (15)$$

$$q_2 = \cos\frac{\phi}{2}\sin\frac{\theta}{2}\cos\frac{\psi}{2} + \sin\frac{\phi}{2}\cos\frac{\theta}{2}\sin\frac{\psi}{2} \qquad (16)$$

$$q_3 = \cos\frac{\phi}{2}\cos\frac{\theta}{2}\sin\frac{\psi}{2} - \sin\frac{\phi}{2}\sin\frac{\theta}{2}\cos\frac{\psi}{2} \qquad (17)$$

and

$$\Omega(\omega) = \frac{1}{2}\begin{bmatrix} 0 & -\omega_x & -\omega_y & -\omega_z \\ \omega_x & 0 & \omega_z & -\omega_y \\ \omega_y & -\omega_z & 0 & \omega_x \\ \omega_z & \omega_y & -\omega_x & 0 \end{bmatrix} \qquad (18)$$

with ω_x, ω_y and ω_z are, respectively, being the roll, pitch and yaw rates of the aircraft. Practically, it is common to use rate gyro measurements to update quaternion estimates. As small-scale UAVs have very limited payload capacity, small micro-electro-mechanical system (MEMS) devices used to measure angular rates usually drift over time. Compensation for the drift is necessary in order to obtain

a reliable estimate. For this reason the state vector is chosen (see, for example, Kingston and Beard (2004)) as

$$x = \begin{pmatrix} q \\ b \end{pmatrix} \tag{19}$$

where b is the estimate of the rate gyro bias, which can be assumed to be slow varying constant and given by

$$b = \begin{pmatrix} b_p \\ b_q \\ b_r \end{pmatrix} \tag{20}$$

and

$$\dot{b} = 0 \tag{21}$$

We thus have

$$\dot{x} = f(x, \omega) = \begin{bmatrix} \Omega(\omega - b) & 0 \end{bmatrix} x + w_x \tag{22}$$

where w_x is the process noise, and it can be shown (see, for example, MathWorks (2009)) that the Euler angles are given by

$$\begin{pmatrix} \phi \\ \theta \\ \psi \end{pmatrix} = \begin{pmatrix} \tan^{-1} \dfrac{2(q_2 q_3 + q_0 q_1)}{1 - 2(q_1^2 + q_2^2)} \\ \sin^{-1}[-2(q_1 q_3 - q_0 q_2)] \\ \tan^{-1} \dfrac{2(q_1 q_2 + q_0 q_3)}{1 - 2(q_2^2 + q_3^2)} \end{pmatrix} \tag{23}$$

In principle, the gyroscope alone is capable of providing attitude information through integration. However, because of the drift, the estimation error resulted from integration increases as time progresses. As such, an attitude determination reference independent of the gyroscope have to be used to correct the resulting error. This can be done by using the measurement signals from accelerometers and magnetometers available in INS with a GPS receiver as follows:

(1) It can be shown that the measurement of the accelerations in the three axes of the aircraft body frame can be expressed as

$$\begin{pmatrix} a_x \\ a_y \\ a_z \end{pmatrix} = -g \begin{pmatrix} -\sin\theta \\ \cos\theta \sin\phi \\ \cos\theta \cos\phi \end{pmatrix} + a_{\text{motion}} = \begin{pmatrix} -2g(q_1 q_3 - q_0 q_2) \\ -2g(q_0 q_1 + q_2 q_3) \\ -g[1 - 2(q_1^2 + q_2^2)] \end{pmatrix} + a_{\text{motion}} \tag{24}$$

where the first term is due to the gravity force (g is the gravity constant) and the second term, i.e. a_{motion}, is related to flight motion, which is negligible compared with

the gravity acceleration for small UAVs and can generally be treated as a measurement noise or disturbance.

(2) The magnetometer provides a reliable measurement for the heading angle ψ by using

$$\psi = \tan^{-1}\frac{m_{x_h}}{m_{y_h}} \tag{25}$$

where m_{x_h} and m_{y_h} are projected magnetic field components on the horizontal plane that can be calculated by transforming the magnetometer measurement vector m as follows

$$
\begin{aligned}
m_{x_h} &= m_x \cos(\phi) + m_y \sin(\theta)\sin(\phi) - m_z \cos(\theta)\sin(\phi) \\
m_{y_h} &= m_y \cos(\theta) + m_z \sin(\theta)
\end{aligned}
\tag{26}
$$

where m_x, m_y, m_z are measured components of magnetic field vector m along the x-, y- and z-axes of body frame, respectively.

This measured ψ, which corresponds to the third equation in (23), can be included as the fourth measurement output for heading angle update.

Finally, we combine (22), the third equation of (23) and (24) to formulate the determination framework for the Euler angles. After the estimation of q_0, q_1, q_2, q_3, we determine the Euler angles using (23).

3. H_∞ filtering design

Based on the position and attitude dynamics derived in the previous section, we carry out the H_∞ filtering design to make an accurate estimation on the aircraft position and attitudes. To be specific, we first briefly introduce the discrete-time H_∞ filtering technique in Section 3.1. Next, we then give the detailed implementations on the estimations of the position and the Euler angles in Sections 3.2 and 3.3, respectively.

3.1   Discrete-time H_∞ filtering

In Kalman filtering, also known as H_2 filtering, the system and measurement noises are assumed to be white with known statistics, and the technique aims at minimizing the variance of the estimation error (see, for example, Kalman (1960)). However, such an assumption is commonly not satisfied in many practical situations such as attitude and position determination. As mentioned earlier, the attitude determination problem is non-linear in nature and its the measurement noise is unknown. It is natural to formulate such a problem as an H_∞ filtering problem.

H_∞ filtering minimizes the 'worst-case' estimation error. Its design objective is to ensure that the energy gain from the noise inputs to the estimation error is less than a certain level (see, for example, Kailath *et al.* (1999), Green and Limebeer (1995) and Zhou *et al.* (1995)). Such a design technique is particularly suitable for the attitude and

position determination problems since it only requires the noise inputs to be deterministic and to be energy bounded (Lewis *et al.*, 2007). To be precise, we consider a system characterized by

$$x_k = Ax_{k-1} + Gw_k$$
$$z_k = Hx_k + v_k \tag{27}$$
$$s_k = Lx_k$$

where $x_k \in \mathbb{R}^n$ are the state vectors, $w_k \in \mathbb{R}^l$ and $v_k \in \mathbb{R}^p$ are the process and measurement noises which are assumed to be deterministic and with bounded energy, $z_k \in \mathbb{R}^p$ is the measurement, and $s_k \in \mathbb{R}^r$ is the signal to be estimated. The H_∞ filtering design consists of the following two stages:

(1) State prediction

$$\bar{x}_k = A\hat{x}_{k-1} \tag{28}$$

where $\hat{x}_{k-1}$ is the estimated state vector in previous step, and $\bar{x}_k$ is the estimated state vector in the prediction stage.

(2) Time update

$$K_k = AP_kH^{\mathrm{T}}(I + HP_kH^{\mathrm{T}})^{-1}$$
$$\hat{x}_k = \bar{x}_k + K_k(z_k - H\bar{x}_k) \tag{29}$$
$$P_{k+1}^{-1} = [A(P_k^{-1} + H^{\mathrm{T}}H)^{-1}A^{\mathrm{T}} + GG^{\mathrm{T}}]^{-1} - \gamma^{-2}L^{\mathrm{T}}L$$

where P_k is the corresponding covariance matrix of x_k at the current step, I is an identity matrix, K_k is the H_∞ filter gain matrix at the current step and $\gamma > 0$ is the level of noise attenuation. The H_∞ filter is capable of yielding an estimate $\hat{s}_k$ of s_k based on the measurements $z_0, z_1, \ldots, z_{k-1}$ for any (x_0, w, v) with x_0 bounded, $w \in \ell_2 [0, N-1]$ and $v \in \ell_2 [0, N-1]$.

Consider the system in (27) and a given $\gamma > 0$, it was shown by Lewis *et al.* (2007) that there exists an H_∞ filter over $[0, N]$ if and only if there exists a solution $P_k = P_k^{\mathrm{T}} > 0$ ($k = 0, 1, \ldots, N$) to the following discrete-time Riccati equation:

$$(P_{k+1}^{-1} + \gamma^{-2}L^{\mathrm{T}}L)^{-1} = A(P_k^{-1} + H^{\mathrm{T}}H)^{-1}A^{\mathrm{T}} + GG^{\mathrm{T}} \tag{30}$$

where $P_0 = P_{x_0}$ is a positive-definite matrix reflecting the uncertainty of the initial state estimate relative to the combined energy of the process and measurement noises. If the condition is satisfied, the H_∞ filter given by (28) and (29) with the filter gain of $K_k = AP_kH^{\mathrm{T}}(I + HP_kH^{\mathrm{T}})^{-1}$ achieves

$$J = \|s - \hat{s}\|_{2,[0,N-1]}^2 - \gamma^2 \left((x_0 - \bar{x}_0)^{\mathrm{T}}P_{x_0}^{-1}(x_0 - \bar{x}_0) + \|w\|_{2,[0,N-1]}^2 + \|v\|_{2,[0,N-1]}^2 \right) < 0 \tag{31}$$

3.2 H_∞ filtering for GPS position signal enhancement

For the GPS position signal enhancement, we discretize the continuous-time system of (27) with a sampling period of 0.02 s. Such a sampling period is used in the hardware system of our UAV helicopter. We obtain

$$
x_k = \begin{bmatrix} 1 & 0.02 \\ 0 & 1 \end{bmatrix} x_{k-1} + \begin{bmatrix} 0.02 & 0 \\ 0 & 0.002 \end{bmatrix} w_k
$$
$$
z_k = [1 \quad 0] x_k + v_k \tag{32}
$$

$$
s_k = x_k
$$

The H_∞ filtering technique described in (28) and (29) is then implemented. Using the result of Chen (2000), we can compute that the best possible choice of γ is given by $\gamma^* = 1.04897$ for this system. However, it requires an infinite gain to achieve such a noise attenuation. For a practical filtering design, we choose $\gamma = 1.23 > \gamma^*$, which yields a satisfactory performance. Note that the initial values for P_0 and x_0 are chosen by

$$
P_0 = \begin{bmatrix} 1 & 0 \\ 0 & 1 \end{bmatrix}, \quad x_0 = \begin{pmatrix} 0 \\ 0 \end{pmatrix} \tag{33}
$$

3.3 H_∞ filtering for euler-angles determination

For the non-linear Euler-angles determination dynamics, we first rewrite its continuous-time dynamics obtained in Section 2.2 as follows:

$$
\dot{x} = f_c(x) + w
$$
$$
z = h_c(x) + v \tag{34}
$$
$$
s = x
$$

where $x \in \mathbb{R}^n$ is the state variable, $z \in \mathbb{R}^p$ is the measurement output, $f_c(x)$ and $h_c(x)$ are sufficiently smooth functions of appropriate dimension, w and v are process and measurement noises or disturbances, assumed to be deterministic and with bounded energy. Its corresponding discrete-time counterpart can be expressed as

$$
x_k = f(x_{k-1}) + Gw_k
$$
$$
z_k = h(x_k) + Vv_k \tag{35}
$$
$$
s_k = x_k
$$

Expanding the nonlinear functions $f(\cdot)$ and $h(\cdot)$ using Taylor series expansion at the filtered $\hat{x}_{k-1}$ and predicted estimates $\bar{x}_{k-1}$, we obtain

$$
x_k = f(\hat{x}_{k-1}) + F_k(x_{k-1} - \hat{x}_{k-1}) + Gw_k
$$
$$
z_k = h(\bar{x}_k) + H_k(x_{k-1} - \bar{x}_{k-1}) + Vv_k \tag{36}
$$

where F_k and G are the Jacobian matrices of partial derivatives of f with respect to x and w, and H_k and V are the Jacobian matrices of partial derivatives of h with respect to x and v. More specifically,

$$F_k[i,j] = \left.\frac{\partial f_{[i]}}{\partial x_{[j]}}\right|_{\hat{x}_{k-1}}, \quad G[i,j] = \left.\frac{\partial f_{[i]}}{\partial w_{[j]}}\right|_{\hat{x}_{k-1}}, \quad H_k[i,j] = \left.\frac{\partial h_{[i]}}{\partial x_{[j]}}\right|_{\bar{x}_{k-1}}, \quad V[i,j] = \left.\frac{\partial h_{[i]}}{\partial v_{[j]}}\right|_{\bar{x}_{k-1}}$$

(37)

Without knowing the individual values of the noise w_k and v_k at each time step, the state and measurement vector can be approximated as

$$\bar{x}_k = f(\hat{x}_{k-1})$$
$$\bar{z}_k = h(\bar{x}_k)$$

(38)

We then substitute (38) into (36), and define the new state vector $\tilde{x}_k$ as

$$\tilde{x}_{k-1} = x_{k-1} - \hat{x}_{k-1} \quad \text{(previous step)}$$
$$\tilde{x}_k = x_k - \bar{x}_k \quad \text{(current step)}$$

(39)

Note that for constructing $\tilde{x}_{k-1}$, we use $\hat{x}_{k-1}$ instead of $\bar{x}_{k-1}$ since the former is the more accurate time-update result. Define a new measurement output $\tilde{z}_k$ as

$$\tilde{z}_k = V^{-1}(z_k - \bar{z}_k)$$
$$\tilde{H}_k = V^{-1}H_k$$

(40)

With (39) and (40), we can give the H_∞-compatible formulation as

$$\tilde{x}_k = F_k\tilde{x}_{k-1} + Gw_k$$
$$\tilde{z}_k = \tilde{H}_k\tilde{x}_k + v_k$$
$$\tilde{s}_k = \tilde{x}_k$$

(41)

Finally, we note that the corresponding Jacobian matrices for the attitude dynamics are given by

$$F_k = \begin{bmatrix} 1 & -(\omega_x - b_p)T & -(\omega_y - b_q)T & -(\omega_z - b_r)T & q_1T & q_2T & q_3T \\ (\omega_x - b_p)T & 1 & (\omega_z - b_r)T & -(\omega_y - b_q)T & -q_0T & q_3T & q_2T \\ (\omega_y - b_q)T & -(\omega_z - b_r)T & 1 & (\omega_x - b_p)T & -q_3T & -q_0T & q_1T \\ (\omega_z - b_r)T & (\omega_y - b_q)T & (\omega_x - b_p)T & 1 & q_2T & -q_1T & -q_0T \\ 0 & 0 & 0 & 0 & 1 & 0 & 0 \\ 0 & 0 & 0 & 0 & 0 & 1 & 0 \\ 0 & 0 & 0 & 0 & 0 & 0 & 1 \end{bmatrix}$$

where T is the sampling period, which is taken as 0.02 s in obtaining the implementation results given in the next section,

$$H_k = \begin{bmatrix} 2gq_2 & -2gq_3 & 2gq_0 & -2gq_1 & 0 & 0 & 0 \\ -2gq_1 & -2gq_0 & -2gq_3 & -2gq_2 & 0 & 0 & 0 \\ -2gq_0 & 2gq_1 & 2gq_2 & -2gq_3 & 0 & 0 & 0 \\ q_3\delta_2\delta_3 & q_2\delta_2\delta_3 & q_1\delta_2\delta_3 + 2q_2\delta_1\delta_3 & q_0\delta_2\delta_3 + q_3\delta_1\delta_3 & 0 & 0 & 0 \end{bmatrix}$$

where

$$\delta_1 = 2(q_1q_2 + q_0q_3), \quad \delta_2 = 1 - 2(q_2^2 + q_3^2), \quad \delta_3 = \frac{2}{[1 - 2(q_2^2 + q_3^2)]^2 + [2(q_1q_2 + q_0q_3)]^2},$$

$$G = \begin{bmatrix} 10^{-4} & 0 & 0 & 0 & 0 & 0 & 0 \\ 0 & 10^{-4} & 0 & 0 & 0 & 0 & 0 \\ 0 & 0 & 10^{-4} & 0 & 0 & 0 & 0 \\ 0 & 0 & 0 & 10^{-4} & 0 & 0 & 0 \\ 0 & 0 & 0 & 0 & 10^{-6} & 0 & 0 \\ 0 & 0 & 0 & 0 & 0 & 10^{-6} & 0 \\ 0 & 0 & 0 & 0 & 0 & 0 & 10^{-6} \end{bmatrix}$$

and

$$V = \begin{bmatrix} 0.981 & 0 & 0 & 0 \\ 0 & 0.981 & 0 & 0 \\ 0 & 0 & 0.981 & 0 \\ 0 & 0 & 0 & 0.1221 \end{bmatrix}.$$

Based on the dynamics given in (41), an H_∞ filter can be constructed as follows:

(1) State prediction

$$\bar{x}_k = f(\hat{x}_{k-1}) \tag{42}$$

(2) Time update

$$\begin{aligned} K_k &= P_k \tilde{H}_k^T (I + \tilde{H}_k P_k \tilde{H}_k^T)^{-1} \\ \hat{x}_k &= \bar{x}_k + K_k(z_k - h(\bar{x}_k)) \\ P_{k+1}^{-1} &= [\tilde{F}_k(P_k^{-1} + \tilde{H}_k^T \tilde{H}_k)^{-1}\tilde{F}_k^T + GG^T]^{-1} - \gamma^{-2}I \end{aligned} \tag{43}$$

where P_k is the corresponding covariance matrix of x_k and K_k is the resulting H_∞ filter gain. It should be noted that it is not possible to use a constant γ for this problem as the Jacobian matrices $\tilde{F}_k$ and $\tilde{H}_k$ are time-varying. A specific γ is required to be

determined in real-time and used for each step. As for the initial states, we take $P_0 = \text{diag}\{0.1, 0.1, 0.1, 0.1, 0.1, 0.1, 0.1\}$ and $x_0 = 0$.

4.   Experimental Results

In this section, we evaluate the practical performance of the designed H_∞ filters. To prove the efficiency of our design, we compare the estimation result with the output data of a commercial product, namely, an NAV420 from Crossbow. Such a product has a GPS-aided AHRS navigation system developed through years of extensive application experience. Its attitude and position estimation is based on Crossbow's self-developed extended Kalman filter algorithm.

Among various flight tests conducted for the GPS signal enhancement, we select a triangle-path flight test as a sample to evaluate the performance of the H_∞ filter we design. The comparison results are shown in Figures 4 and 5. The result clearly shows that with the enhancement of the GPS signals, the problem of jumping in the position
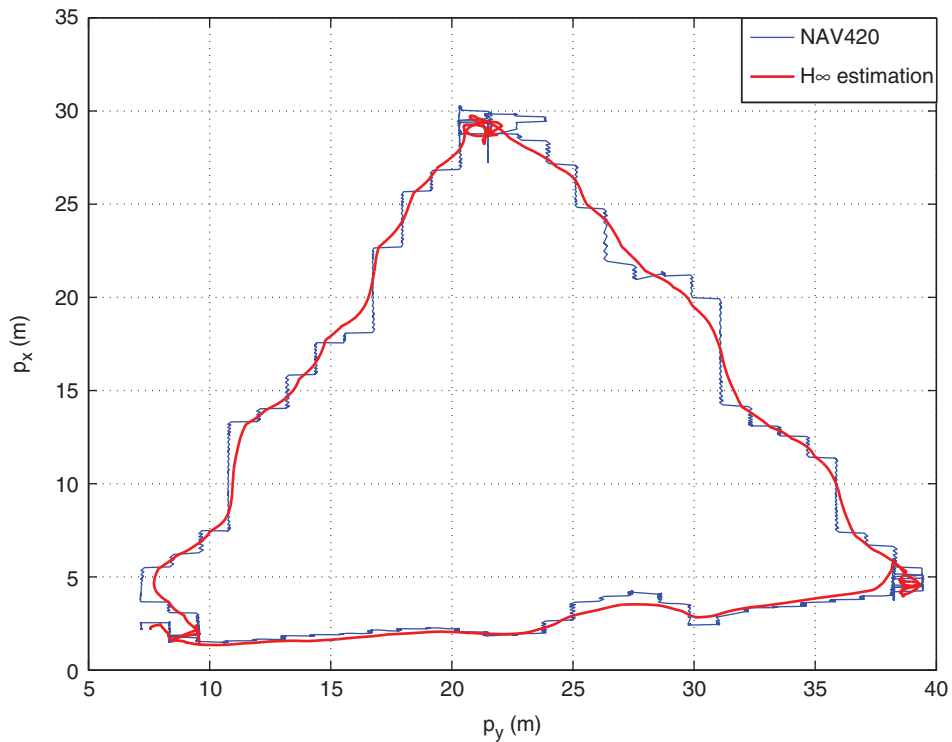
Figure 4 Comparison of the *x–y* position estimated by H_∞ filter (bold line) and that measured by NAV420 (thin line)
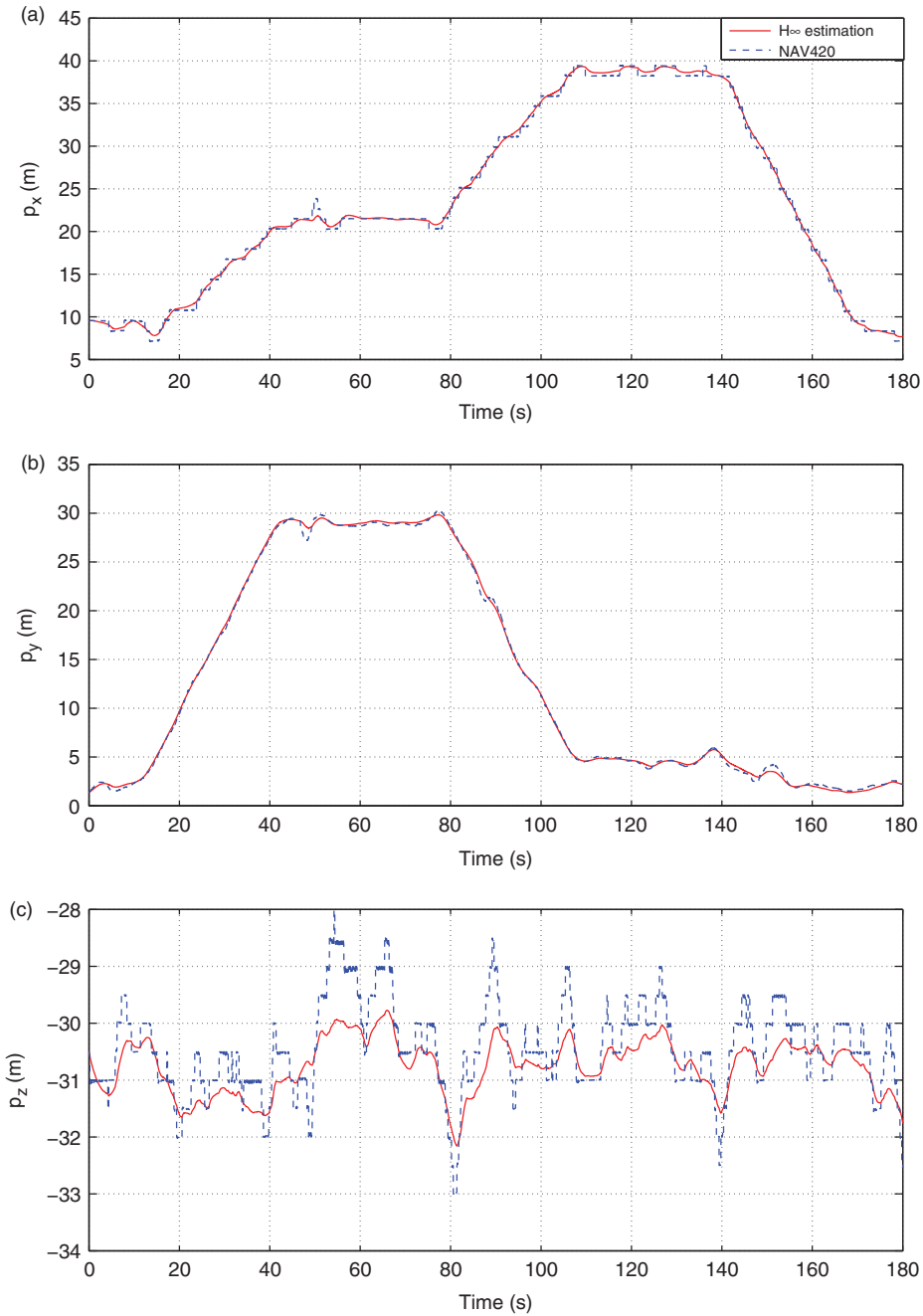
Figure 5 Comparison of the position estimated by H_∞ filter (solid line) and that measured by NAV420 (dashed line): (a) body-frame x-axis position signal; (b) body-frame y-axis position signal; (c) body-frame z-axis position signal
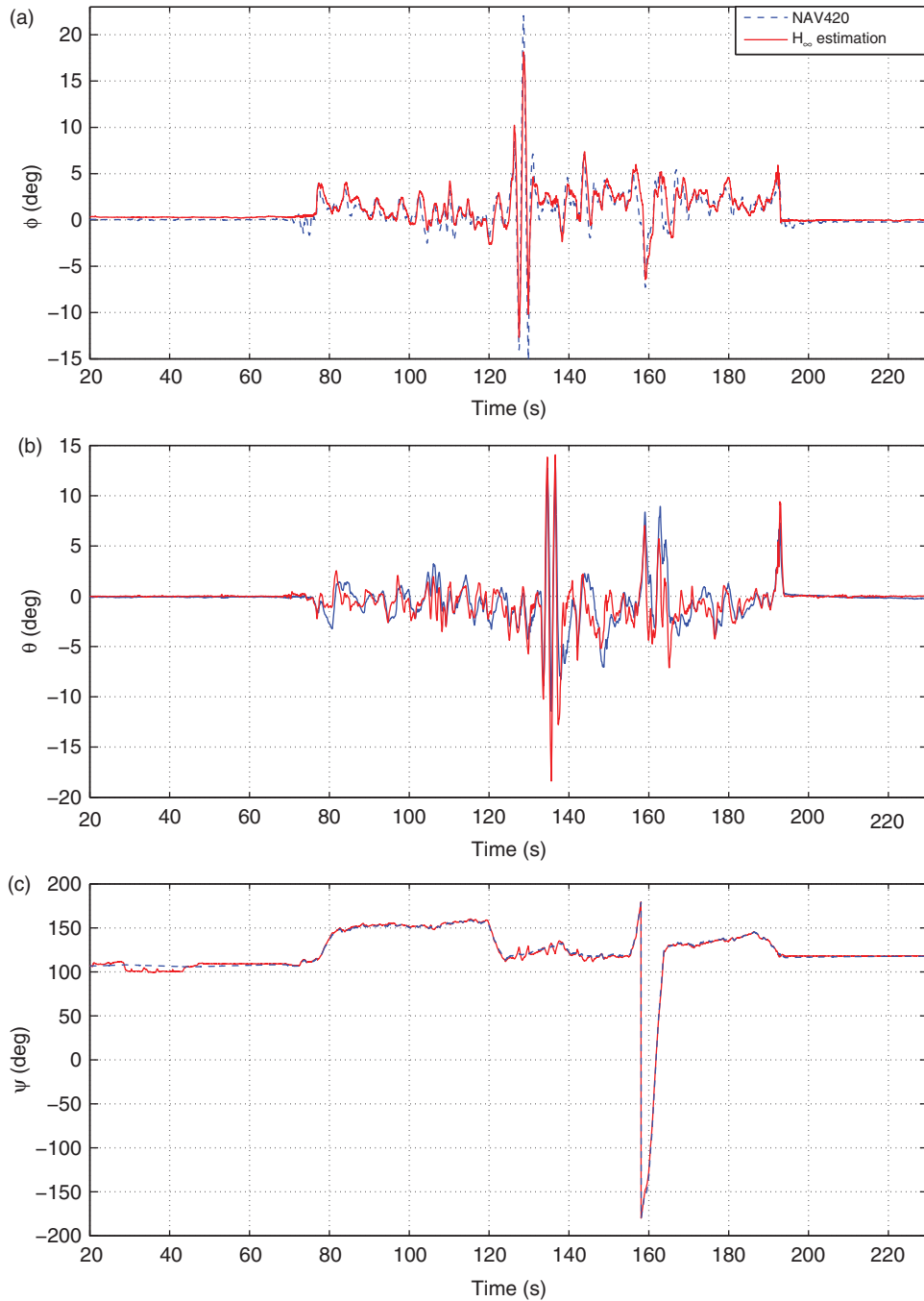
Figure 6 Comparison of Euler angles estimated by H_∞ filter (solid line) and those estimated by NAV420 (dashed line): (a) roll angle; (b) pitch angle; (c) yaw angle

signals has been successfully resolved. Furthermore, the high frequency noises in the GPS position signals are totally eliminated.

The result for the Euler-angles determination is depicted in Figure 6. It can be noted that with the H_∞ filter, the attitude estimation responds more quickly. Furthermore, it provides a faster estimation than the algorithm adopted by NAV420. The estimated result is flatter when the UAV is stationary, while the attitude estimation from NAV420 needs a longer time to converge. Again, the result indicates the obtained H_∞ filter for Euler-angles determination is very satisfactory.

5.   Conclusion

A low-cost attitude determination and navigation optimization system has been investigated in this paper. We have obtained a better attitude measurement with fast response and with no estimation bias using the recently developed H_∞ filtering technique. The experimental results have shown that such a scheme is very effective. The design has been implemented and used on our UAV system to provide reliable measurement for conducting various automatic flight control systems.

References

Britting, K.R. 1971: *Inertial Navigation System Analysis*. Wiley, New York.

Caruso, M.J. 1997: Application of magnetoresistive sensors in navigation systems. *Sensors and Actuators* 1220, 15–21.

Caruso, M.J. 2000: *Applications of Magnetic Sensors for Low Cost Compass Systems*. Technical Report, Honeywell.

Chen, B.M. 2000: *Robust and H_∞-Control*. Springer, London.

Green, M. and **Limebeer, D.J.N.** 1995: *Linear Robust Control*. Prentice-Hall, Englewood Cliffs, NJ.

Kalman, R.E. 1960: A new approach to linear filtering and prediction problems. *Transactions of the ASME – Journal of Basic Engineering* 82, 35–45.

Kailath, T., **Sayed, A.H.** and **Hassibi, B.** 1999: *Linear Estimation*. Prentice-Hall, Upper Saddle River, NJ.

Kingston, D.B. and **Beard, R.** 2004: Real-time attitude and position estimation for small UAVs using low-cost censors. *AIAA 3rd Unmanned Unlimited Technical Conference, Workshop and Exhibit*, Chicago, IL, Paper AIAA, 2004–6488.

Lewis, F.L., **Xie, L.** and **Popa, D.** 2007: *Optimal and Robust Estimation*. 2nd edition. CRC Press, New York.

MathWorks 2009: *Euler Angles to Quaternions*. Technical Document. Accessed September 2009 at: http://www.mathworks.com

Nassar, S., **Schwarz, K.P.** and **El-Sheimy, N.** 2004: INS and INS-GPS accuracy improvement using autoregressive (AR) modeling of INS sensor errors. *Proceedings of the ION 2004 National Technical Meeting*. San Diego, CA, 936–44.

Noureldin, A., **Sharaf, R.**, **Osman, A.** and **El-Sheimy, N.** 2004: INS/GPS data fusion technique utilizing radial basis functions neural networks. *Proceedings of IEEE Position, Location and Navigation Symposium*. Monterey, CA, 280–4.

Shin, E.H. and **El-Sheimy, N.** 2002: Optimizing smoothing computation for

near real-time GPS measurement gap filling in INS/GPS systems. *Proceedings of the Institute of Navigation GPS*, 1434–41.

Tsach, S., **Penn, D.** and **Levy, A.** 2002: Advanced technologies and approaches for next generation UAVs. *Proceedings of International Council of the Aeronautical Sciences Congress,* 131, 1–10.

van der Merwe, R. and **Wan, E.A.** 2004: Sigma-point Kalman filters for nonlinear estimation and sensor-fusion: applications to integrated navigation. *Proceedings of the AIAA Guidance, Navigation Control Conference*, Providence, RI, 16–19.

Wertz, J.R. (ed.) 1978: *Spacecraft Attitude Determination and Control*. D. **Reidel**, Dordrecht.

Zhou, K., **Doyle, J.C.** and **Glover, K.** 1995: *Robust and Optimal Control*. Prentice-Hall, Upper Saddle River, NJ.